



Identification of sediment–basement structure in West Papua province, Indonesia, using gravity and magnetic data inversion as an Earth's crust stress indicator

Richard Lewerissa¹ · Sismanto² · Laura A. S. Lapono³

Received: 18 December 2021 / Accepted: 22 August 2022

© The Author(s) under exclusive licence to Institute of Geophysics, Polish Academy of Sciences & Polish Academy of Sciences 2022

Abstract

West Papua province in eastern Indonesia is positioned in a dynamic tectonic zone along with the collision of the Australian, Pacific, and Eurasian plates. The interaction resulted in the formation of strike-slip faults such as Koor, Sorong, Ransiki, and Yapen, that are prone to earthquakes in the region. The rocks of West Papua in the northern part are a contribution to the Pacific Ocean plate consisting of ophiolite and volcanic arcs of the archipelago, even while the rocks of the Australian plate in the southern part are dominated by quaternary and siliciclastic sedimentary. It has a wide variety of resources, including oil and gas. This study combines the interpretation of regional gravity and magnetic data derived from satellite observations to identify the subsurface structure of West Papua. This is performed since most studies were conducted on the surface and did not significantly focus on the subsurface. The composition of subsurface is determined through three-dimensional (3-D) unconstrained inversion modeling using the iterative reweighting inversion of regional gravity and magnetic anomalies as a function of density contrast and magnetic susceptibility of rocks. In depth variations, gravity inversion produces density contrast ranging from -0.348 to 0.451 gr/cm^3 , whereas magnetic inversion provides rock susceptibility varying between -0.363 and 0.223 SI. Gravity and magnetic inversions characterize the subduction of the Pacific Ocean plate in the north, extensive intrusion of igneous rocks, and low density-susceptibility contrast in the Bintuni basin as a source of oil and natural gas. The boundary between the sediment layer and the basement is believed to be 15–20 km deep, with rocks from the uplifted mantle in the north and a Silur-Devon aged Kemum formation in the south.

Keywords Gravity and magnetic · Inversion modeling · Sediment · Basement · West Papua

Introduction

The west region of Papua Island is administratively one of a provinces in Indonesia. Tectonically, this island is one of a most complex zones at the convergence boundary of Australian and Pacific plates, also is at the forefront of understanding the overall tectonic process on Earth (Baldwin et al. 2012). The Manokwari trough, located on the northern region of West Papua province, is a subduction boundary of the Caroline-Pacific oceanic crust beneath the Australian continental crust. The trough is considered to become a source of seismic activity in Papua's Bird's Head region, which is connected to major strike-slip faults like Sorong and Ransiki (Daniarsyad and Suardi 2017; Lewerissa et al. 2021). There were 2807 earthquakes with magnitudes ranging from 3.5 to 7.7 between 1964 and 2021, most of which were shallow earthquakes, while several large earthquakes caused significant damage in the area.

Edited by Prof. Ivana Vasiljević (ASSOCIATE EDITOR) / Prof. Michał Malinowski (CO-EDITOR-IN-CHIEF).

✉ Richard Lewerissa
r.lewerissa@unipa.ac.id

¹ Department of Physics, Faculty of Mathematics and Natural Sciences, Papua University, Manokwari, Papua Barat 98312, Indonesia

² Department of Physics, Faculty of Mathematics and Natural Sciences, Universitas Gadjah Mada, Yogyakarta 55281, Indonesia

³ Department of Physics, Faculty of Sciences and Engineering, Nusa Cendana University, Nusa Tenggara Timur, Kupang 85148, Indonesia

An earthquake hazard study is essential for determining the characteristics of future earthquake-prone sites and preventing the negative impacts on civilization (Kalaneh and Agh-Atabai 2016).

Previously, several seismic and geoscience studies in the West Papua region were conducted, including determining the source mechanism of the 6.7 Mw earthquake at Ransiki in 2012 (Serhalawan and Sianipar 2017), fault studies to evaluate quaternary activity and indications of seismic hazard in West Papua (Watkinson and Hall 2017), and mapping of seismic hazard on Papua Island in two regions, including Indonesia and Papua New Guinea using probabilistic seismic hazard analysis (PSHA) (Makrup et al. 2018). Furthermore, terrane gravity and tectonic measurements have been taken in a New Guinea indicating that the gravity method is an essential approach for terrane analysis but cannot be employed for isolated structures (Milsom 1991). According to the information, the research that has been conducted is still restricted to studies on the ground surface and has not thoroughly investigated the subsurface structure. Our research employs a potential field of geophysical methods with the objective of understanding and identifying the structure of sediments and basements derived from satellite gravity and magnetic data availability. A study was carried out to determine the stress level of the crust in West Papua.

In 2021, we evaluated the variance in a magnitude of completeness (M_c) and b value in West Papua from the USGS and ISC earthquake catalogs from 1960 to 2021. M_c is an essential variable in seismicity research since it represents the minimum magnitude in the entire earthquake recording. The b value is a tectonic parameter based on the slope of the magnitude distribution to the earthquake frequency. The value of b for the West Papua area is moderate, indicating that this parameter is connected with stress and strain changes, faults, and deformation rates. High crustal stress is indicated by a low b value and vice versa (Lewerissa et al. 2021). Geophysical data are significant in the prediction and evaluation of earthquake hazards, which provide information on the geological structure of the crust. Gravity data contribute to the invention of crust and lithosphere models at various scales, revealing the density distribution of the top layers. On the other hand, it improves knowledge of the basin as a source of oil, gas, and water, and also detects key tectonic features or structures (Saibi et al. 2021). Differences in crustal density are frequently associated with tectonic features and faults, which show a geological framework for seismic risk study. The density of each layer that makes up the Earth is critical for many investigations, including earthquake studies, tectonic plate reconstruction, and modeling the petroleum system (Gómez-García et al. 2019; Tian et al. 2020). In the study area, there are two main basins producing the largest amounts of oil and natural gas in eastern Indonesia, including the Salawati and Bintuni basins.

Satellites can detect fluctuations in a geomagnetic field generated by various geological characteristics of the lithosphere. A magnetic anomaly maps can provide critical information about tectonic structures and the lithosphere in general. Gravity and magnetic remote sensing techniques are relatively inexpensive, non-invasive, and non-destructive. Furthermore, they provide information about the density and variation of the magnetic susceptibility of rocks. This research examines the use of Earth's gravity gradient in the form of vertical, horizontal, and tilt angle derivatives to identify the borders of geological formations such as major faults. The sedimentary and basement layer are derived from an inversion of gravity and magnetic anomalies. These findings are expected to support disaster mitigation or the search for new natural resources in West Papua region.

Geology and tectonic setting

New Guinea, also known as Papua Island, is defined as having the shape of a bird from west to east, with a head, neck, body, and tail. The bird's head, tail, and part of its body can be found in Indonesia's Papua and West Papua, while the rest of the tail can be found in Papua New Guinea (Gold et al. 2017b). Regionally, Papua Island is influenced by two main activities that collide simultaneously until now. The Pacific plate is moving southwest relative to the Australian plate at a speed of 11 cm/year, resulting in a complex tectonic structure (Handyarso and Padmawidjaja 2017).

The neck is largely composed of limestone and siliciclastic that were shortened during the creation of the Lengguru fold belt. This rock is deformed and part of the mountain belt that extends from the west of New Guinea (bird's head), along the Lengguru fold, and then into the central mountains to the end of the eastern island. The rocks in the south of the island of Papua are derived from the Australian continental plate, while the northern part consists of the ophiolite and volcanic arc of the archipelago of the Pacific plate, which is separated by sediment slices in the middle, as well as variations of metamorphic and granite (Fig. 1).

This alignment is characterized by the presence of sutures formed during arc and continental collisions in the Oligocene and early Miocene. The Ransiki fault, located to the east of the bird's head, is thought to be due of a collision between an island arc and Australian continent, restricting into Cenderawasih Bay, east of Wandamen, and connecting with the Weyland overthrust in a Central Mountains (Gold et al. 2017a; Milsom 1991; Milsom et al. 1992). Currently, the dominant arc rock forms the basement at the northern margin of Papua, the eastern bird's head, Cenderawasih Bay, and its islands. The Ransiki Fault is estimated to be a dextral shear zone with a NNW trend, connecting the Sorong Fault and the Yapen Fault, estimated to be inactive (Charlton

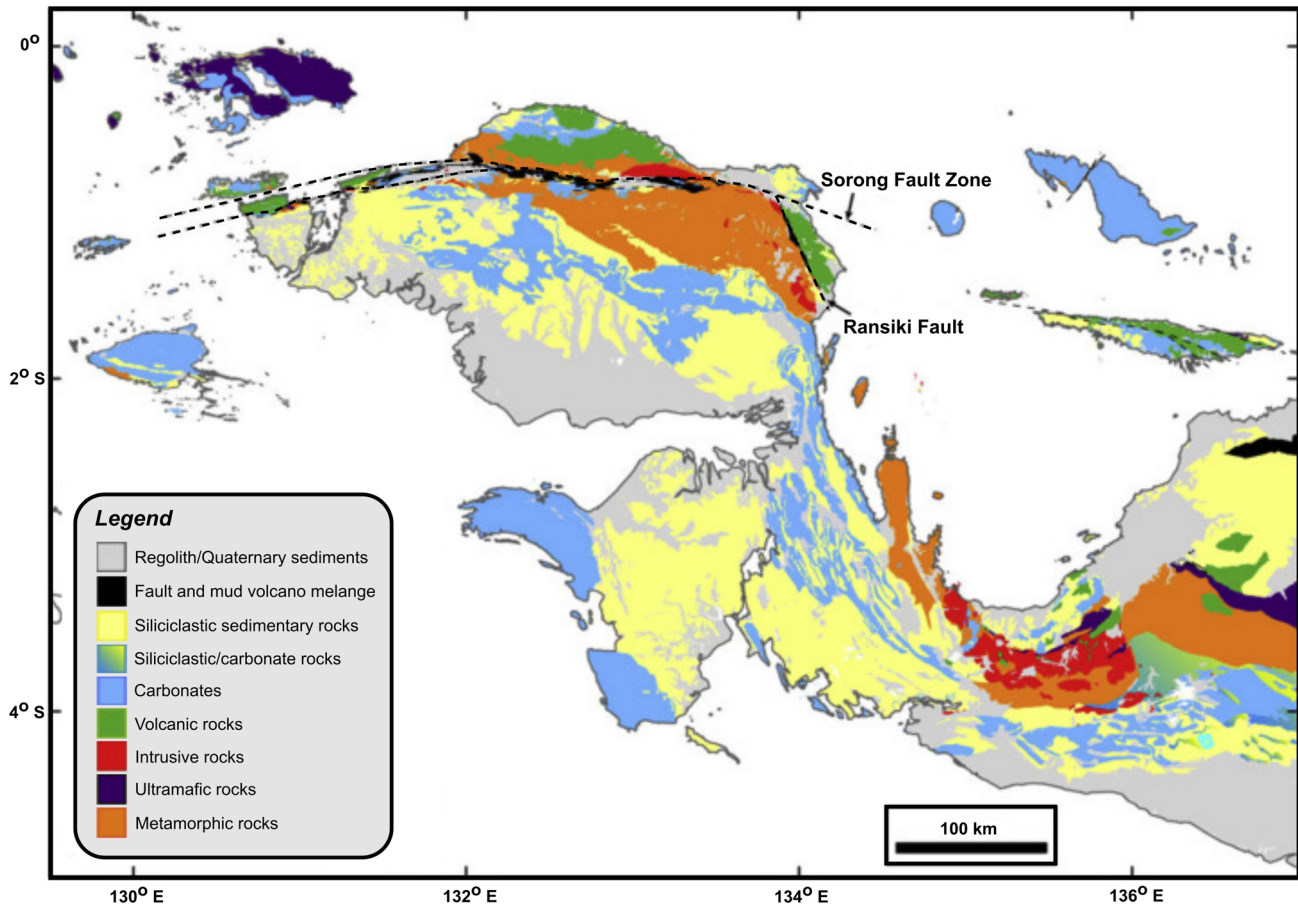


Fig. 1 Lithological map of western Papua, Indonesia, depicting the main fault structure, dominated by volcanic, metamorphic, and sedimentary rocks (Gold et al. 2017b)

2010). The length of a typical segment of this fault ranges from 20–50 km, while the maximum is around 100 km (Watkinson and Hall 2017).

Methodology

Our study looks at the bird's head region in the Indonesian province of West Papua, which has unique and complex tectonic features. The coordinates of the research area are between 131° E–135° E and 0°–4° S, which is an area that is prone to earthquakes caused by collision of the Australian, Pacific, and Eurasian plates, as well as several other microplates.

The historical seismic data from 1960 to 2021 obtained from the IRIS Data Management Center (<http://service.iris.edu/fdsnws/event/1>) show that earthquakes mainly occurred in Koor, Sorong, Ransiki, and Yapen (Fig. 2). This study integrates the interpretation and combination of regional gravity and magnetic potential field data based on satellite

measurements to obtain the subsurface structure of West Papua.

The gravity data come from the 2012 World Gravity Map (WGM), and it contains free air and complete Bouguer anomaly (Balmino et al. 2012; Lewerissa et al. 2020). Gravity data were obtained from the World Gravity Map (WGM) in the form of free air and complete Bouguer anomalies in 2012 (Balmino et al. 2012; Lewerissa et al. 2020). Second vertical derivative data are derived from the XGM2019e model (Zingerle et al. 2020), whereas magnetic data are derived from the NOAA Earth Magnetic Anomaly Grid 2 version 3 (EMAG2-v3) with a spatial resolution of two arc minutes (Lewerissa et al. 2020; Meyer et al. 2017). Moreover, the Global CRUST 1.0 is used as a constraint in 3-D gravity and magnetic inversion (Laske et al. 2013).

Gravity data

The study utilizes the Earth's gravity method for mapping and delineating sedimentary and basement structure boundaries in a West Papua using satellite gravity data

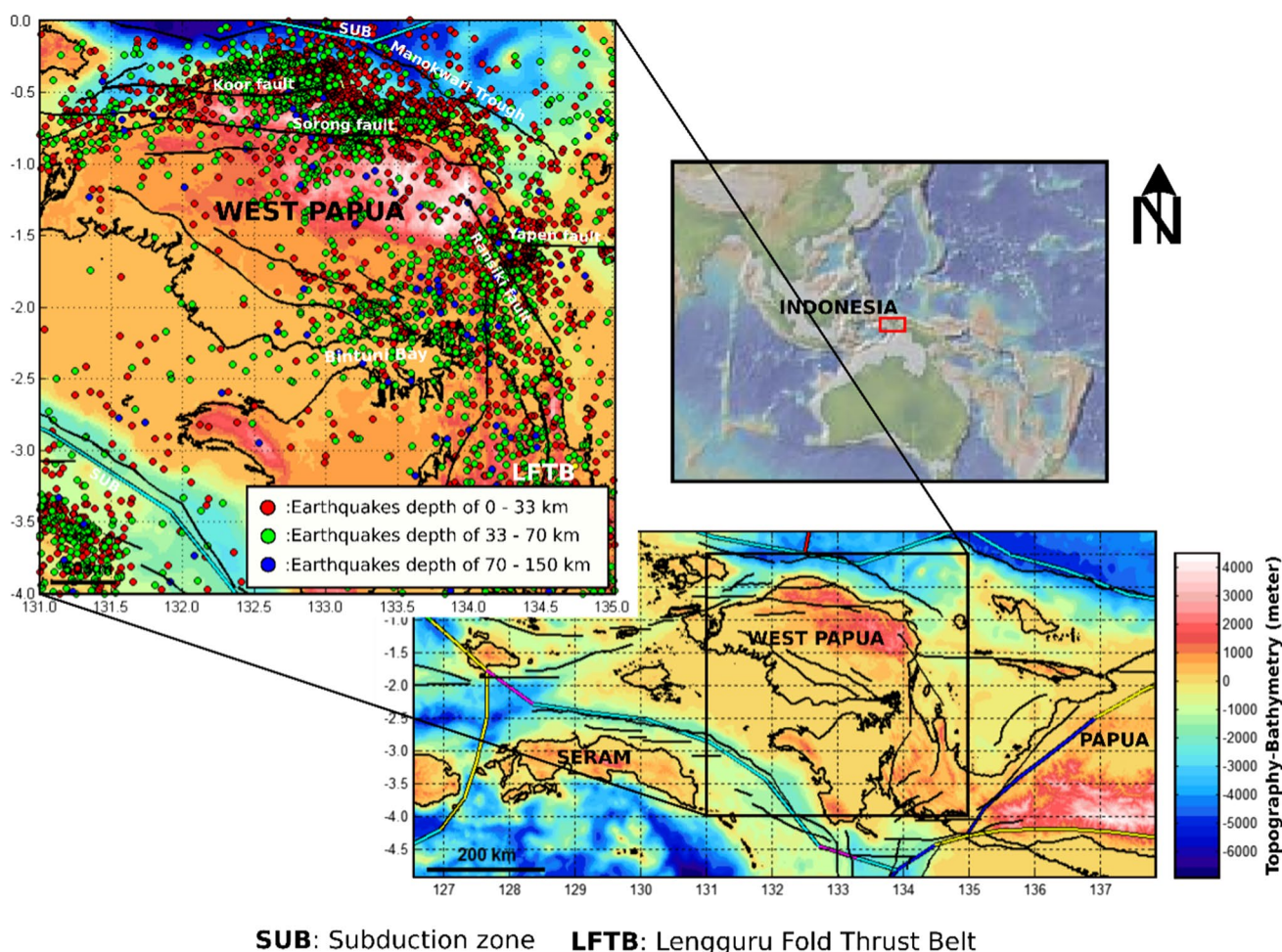


Fig. 2 The study area of Bird Head in West Papua province, Indonesia. It is covered with topography and bathymetry maps, and the main fault structures are the Sorong, Koor, Ransiki, and Yapen

from the 2012 WGM model. Global gravity fields can be measured via satellite, which can reach areas where direct measurement is expensive and time-consuming as in the sea (Gómez-García et al. 2019). WGM 2012 is a worldwide grid map of high-resolution gravity anomalies computed using spherical geometry. The gravity model is produced using the global Earth gravity EGM2008 and DTU10, including the correction of the ETOPO1 with a $1' \times 1'$ resolution field, taking into account the contribution of most surface masses (Balmino et al. 2012). Figure 3 shows free air and complete Bouguer anomalies in West Papua depending on the 2012 WGM model. Additionally, XGM2019e is a model of an integrated global gravity field with a spatial resolution of 2 arc minute (4 km) represented by spherical harmonics of degrees and orders up to 5399. The model consists of the GOCO06s satellite model with wavelength ranges of up to degrees and order of 300, combined with a gravity grid model on the surface covering short wavelengths (Zingerle et al. 2020). Surface

data consist of gravity anomalies on land and ocean provided by the NGA with a resolution of $15'$, plus topographically derived gravity information above the ground (EARTH2014). We use static model calculations from an International Center for Global Earth Model (ICGEM) to obtain a second radial derivative model (Ince et al. 2019) to define the boundaries of regional geological structures in the West Papua region (Fig. 3c). Second radial derivative is an effective filter for enhancing short-wavelength components of gravity anomalies field, associating with structures near the surface and identifying shallow anomalous sources. The zero value of the second-order derivative generally relates to the edge of the source (Dentith and Mudge 2014; Hinze et al. 2013).

As a result, using the upward continuation technique, the complete Bouguer anomaly was separated to generate regional and local anomalies. This approach is used to distinguish regional gravity anomalies caused by deep and massive sources of measured gravity (Zeng et al. 2007).

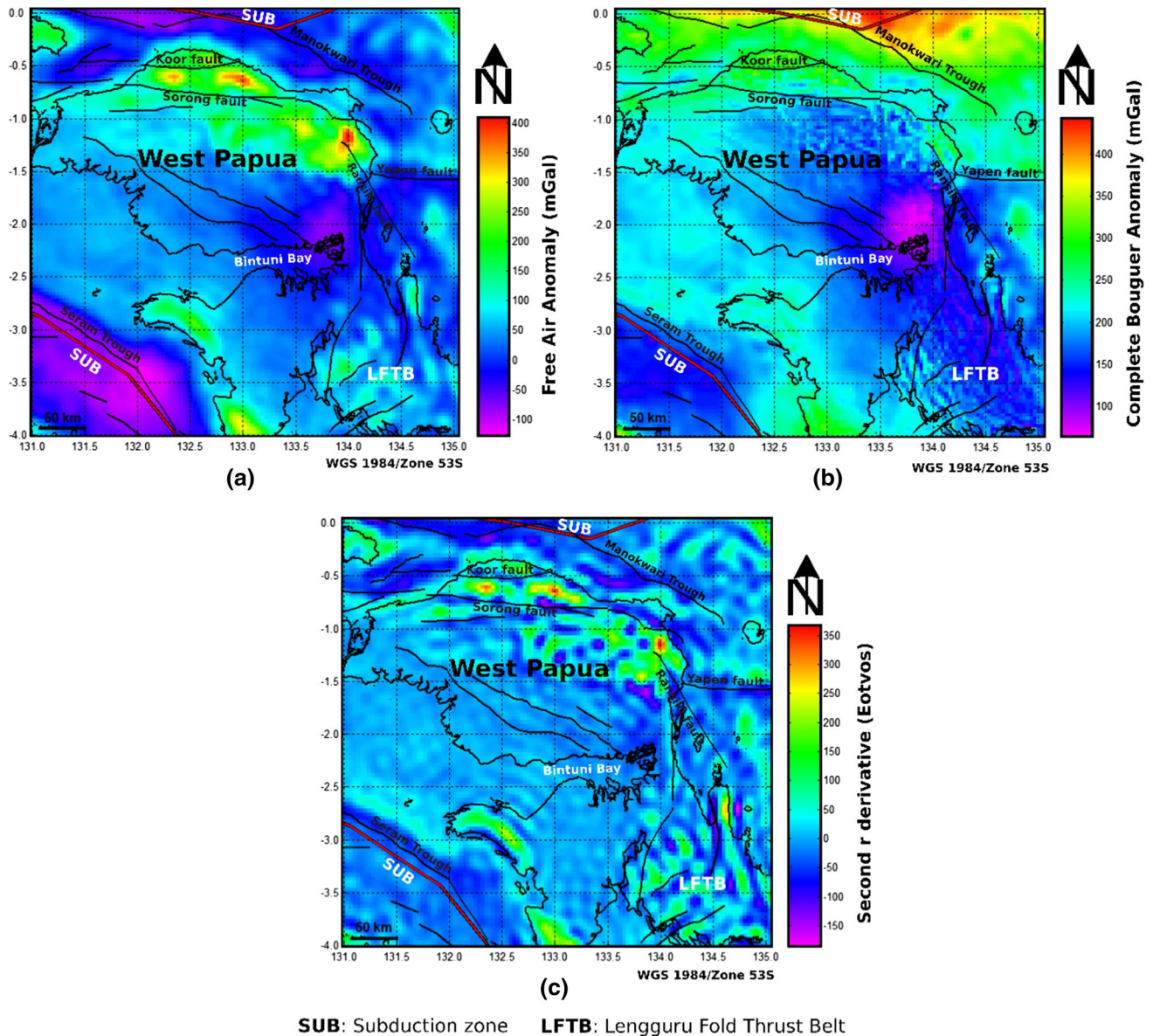


Fig. 3 WGM 2012 and XGM2019e anomalies of Bird's Head region in West Papua province. **a** Free air anomaly; **b** Complete Bouguer anomaly; **c** Second radial derivative

Upward continuation is very simple since projections are often done to free space, which serves to attenuate anomalies with short wavelengths as well as lower the amplitude and noise of the data (Reynolds 1997). According to the EMAG2-v3 upward continuation data, upward continuation of gravity data is conducted at a maximum altitude of 4 km above the surface. Regional gravity anomalies are often utilized as input data for 3-D inversion modeling.

Magnetic data

The magnetic data for the study are based on the NOAA EMAG2-v3 model, which is a collection of magnetic

observations from satellites, ships, and airplanes. EMAG2-v3 is an improved model of the World Digital Magnetic Anomaly (WDMA) map, with 2 arc minutes spatial resolution raised from 3 arc minutes and two sets of data, including magnetic anomalies at sea level and upward continuation at an altitude of 4 km from geoid reduction from 5 km (Maus et al. 2009; Meyer et al. 2017).

EMAG2-v3 data in West Papua region are obtained from Geoscience data service from Geosoft Seequent which provides access to Geosoft Public DAP Server (<https://public.dap.seequent.com/GDP/Search>), in the form of anomalies at sea level (Fig. 4a) and upward continuation anomalies (Fig. 4b). The EMAG2-v3 model is useful as synoptic

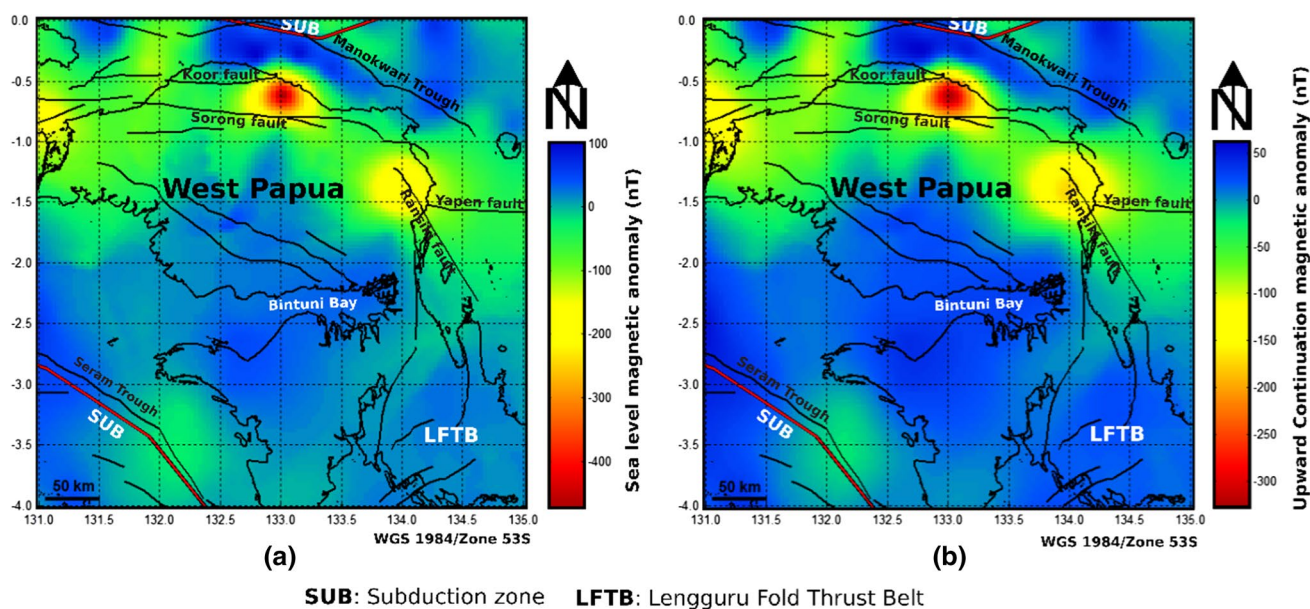


Fig. 4 EMAG2-v3 anomalies in West Papua province: **a** at sea level; **b** at 4-km altitude of upward continuation

information of magnetic fields and repeated measurements of overlapping orbits are used to minimize the ionosphere's foreign magnetic field from lithosphere anomalies. These measurements are made to provide important information about the nature and history of other terrestrial objects (Hinze et al. 2013). The upward continuation magnetic data at an altitude of 4 km are then used as the main data in the inversion modeling without first reduction to pole (RTP), because the study area is large enough that it will experience distortion in the application of RTP.

Gravity field gradient

The gradient method of a gravity field, such as vertical, horizontal, and tilt angle derivatives, is used in this study to enhance near-surface geological features that are not yet visible on a complete Bouguer anomaly of West Papua. Gradient approaches employ vertical and horizontal derivatives to characterize the edges of geological formations and source materials preserved in gravity fields. Vertical gradient is commonly utilized highlight near-surface of geological structure and increase a component of wavenumber spectrum, with a zero value corresponding to the geological structure's boundary (Ibraheem et al. 2019). The vertical gradient equation is written as:

$$VG = \frac{\partial g}{\partial z}. \quad (1)$$

Density contrast boundaries of the gravity field data are determined using a horizontal gradient. When compared to

vertical gradient, this approach is more effective for depicting shallow or deep sources (Abderbi et al. 2017). 2-D horizontal gradient equation is shown as:

$$HG(x, y) = \sqrt{\left(\frac{\partial g}{\partial x}\right)^2 + \left(\frac{\partial g}{\partial y}\right)^2}, \quad (2)$$

g is complete Bouguer anomaly. Another analysis conducted on gravity field data in the West Papua region is tilt angle (TA). This technique is applied to enhance and sharpen the anomalous form of gravity or magnetic. Tilt angle is defined as a ratio of vertical and horizontal derivatives that ranges from -90° to 90° :

$$TA = \tan^{-1} \left(\frac{VG}{HG(x, y)} \right). \quad (3)$$

TA is positive above the sources, close to zero or zero characterizing the source boundary, and negative values are generally outside the source (Eshaghzadeh et al. 2018; Ibraheem et al. 2019). Overall, the gravity field gradient in the study area was calculated using a 2-D fast Fourier transform by Fourpot software (Shandini et al. 2018).

Inversion modeling of potential field data

Gravity and magnetic anomaly inversion modeling was conducted to obtain subsurface structures in West Papua in the form of rock density and susceptibility distribution. Inversion is a numerical computational process used to create subsurface models of physical properties (density and

magnetic susceptibility) that create the same signals seen in the measured gravity and magnetic data (Saibi et al. 2021). This research utilizes the VOXI Earth Modeling facility from Geosoft Oasis Montaj version 9.10 for 3-D inversion in West Papua (Fig. 5a). VOXI Earth Modeling is a cloud and clustered computing module that enables 3-D geophysical inversion include gravity and magnetic. It uses the Cartesian Cut Cell (CCC) inversion approach established by (Ingram et al. 2003), which has been simplified further by (Ellis and MacLeod 2013) to more precisely reflect the surface of geology (Soulaïmani et al. 2020). As a sensor network, we used regional gravity and magnetic anomalies grid and then defined the elevation sensor using a digital elevation model (DEM) and determined the number of samples per cell.

The model sensitivity to fitting the data is then improved until the difference between the predicted data and the measurement data is less than the fit threshold. We created a 3-D model of density and susceptibility contrast using unconstrained inversion procedure on VOXI modeling tools. The constraint iterative reweighting inversion (IRI) was applied to improve the model and produce better geological inversion solutions. In VOXI, the IRI approach is used to sharpen and improve inversion output. IRI not only sharpens inversion, but it also enhances geometry modeling and physical property amplitude recovery (Geosoft 2012). The standard deviation of the data utilized is normally 5%, with gravity data of 2.28 mGal and magnetic data of 2.008 nT. The global settings of regularization auto-fit for data are determined at 1, show the chi-squared misfit, meaning sum-of-squares of predicted minus observed data divided by estimated uncertainties, and divided by a number of data. If the result ~ 1 , it is a good inversion. Furthermore, we set the default values of the important parameters of the inversion controller on VOXI Earth modeling for density and susceptibility constraints, including reference model 0; upper

bounds model $1e+20$; lower bounds model $-1e+20$; weighting model 0.0001; reweighting model 1; and IRI Focus Factor 2. IRI Focus allows for model development and emphasizes the positive and negative ends of the density and susceptibility distributions. Positive values are associated with anomalies due to basement rocks, while negatives are associated with weak zones or alterations, as well as thick sediment layers. Modeling begins with the construction of the reference model in discrete cells of $180 \times 178 \times 17$ in the x , y , and z directions, with a cell size of 2.5 km in x and y directions, while for z it is 2.9 km (Fig. 5b).

In this research, we employed the inversion of physical variables proposed by Li and Oldenburg (1996) for magnetic data and Li and Oldenburg (1998) for gravity data. The method divides the research region into a sequence of rectangular cells, each with a fixed set of physical constants. To summarize, such systems may be stated as:

$$Gm = d, \quad (4)$$

where d is a vector data representing n measurements ($d_{\text{obs}} = [d_1 d_2 d_3 \dots d_n]^T$), G is the sensitivity matrix $N \times M$, where N is the number of data and M the number of model parameters, m ($m = [m_1 m_2 m_3 \dots m_n]^T$) is a vector showing the model's physical attributes for susceptibility or density (Afshar et al. 2018; Oldenburg and Li 2005). In this study, the problem of inversion is underdetermined because the number of cells is greater than the amount of data ($m \gg n$), so it requires additional information to overcome ambiguity. The underdetermined case is formulated as an optimization involving an objective function $\varphi(m)$, combines a data misfit measure (φ_d), and an objective function model ($\varphi_m(m)$), with a regularization factor (μ), as Tikhonov general as Afshar et al. (2018):

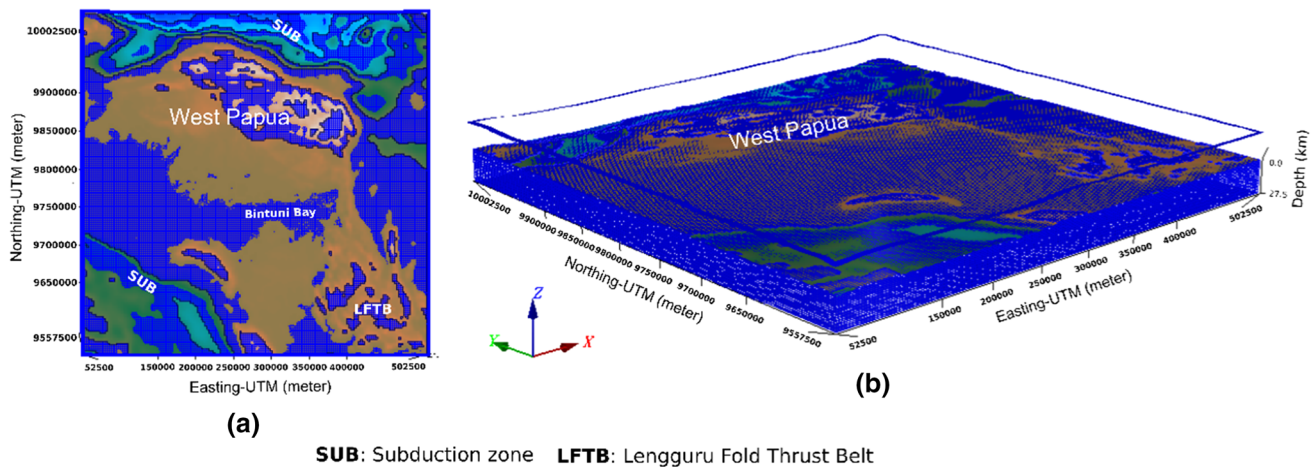


Fig. 5 3-D reference model for the West Papua region: **a** digital elevation model; **b** 3-D grid model in the x , y , and z directions (blue lines indicate model boundaries)

$$\varphi(m) = \varphi_d + \mu\varphi_m(m). \quad (5)$$

The data misfit function is:

$$\varphi_d = \|W_d(Gm - d^{\text{obs}})\|^2, \quad (6)$$

where $W_d = \text{diag}[1/\sigma_1 \dots 1/\sigma_n]$ and σ_i is the standard deviation of error associated with the i th datum. φ_d is quite small for acceptable model.

The model objective function, which is based on two terms, including the smallest difference between the result and the reference model, as well as the roughness constraints of the inversion model in all three directions, is expressed as Li and Oldenburg (1996):

$$\varphi_m(m) = \alpha_s \|W_s(m - m_{\text{ref}})\|^2 + \alpha_x \|W_x(m - m_{\text{ref}})\|^2. \quad (7)$$

m_{ref} is the reference model, W_s and W_x are the weighting matrices of the smallest and flattest models, and α_s and α_x are important controlling coefficients of the proximity of the model to the reference model (Afshar et al. 2018; Oldenburg and Li 1994).

The gravity and magnetic anomalies used as measurement data are upward continuation anomalies at an altitude of 4 km from the surface with an objective to determine the main sediment–basement structures in the region. The total magnetic field, inclination, declination attributes are 40,433.16 nT, -20.14° , and 1.95° , respectively, located at

the midpoint of the West Papua region. The research area is 4° square, and for inversion modeling, the data are transformed from geographical coordinates to UTM so that the curvature factor can be minimized. This study also examined the CRUST 1.0 global crust model as a restriction on gravity and magnetic data inversion modeling. CRUST 1.0 has a resolution of $1^\circ \times 1^\circ$ and includes data on global surface topography, seabed bathymetry, seismic refraction, ice sheet, sediment, and Earth's crust thickness (Laske et al. 2013; Lewerissa et al. 2020). From CRUST 1.0 model, the maximum crust depth used reaches 30 km; it is estimated that the boundary of the lower crust and mantle in the study area.

Sequent Geosoft gives access to the Geosoft Public DAP Server, which contains data on the subsurface density and thickness of the Earth's crust (<https://public.dap.sequent.com/GDP/Search>), as seen in Fig. 6a, b.

Result and discussion

Gravity anomalies separation in West Papua

Free air anomaly in West Papua based on the 2012 WGM model ranges from -127.64 to 410.12 mGal (Fig. 3a), while the complete Bouguer anomaly is of positive value between 63,830 and 443.82 mGal covering land and ocean (Fig. 3b). Low free air anomalies are found in the northern

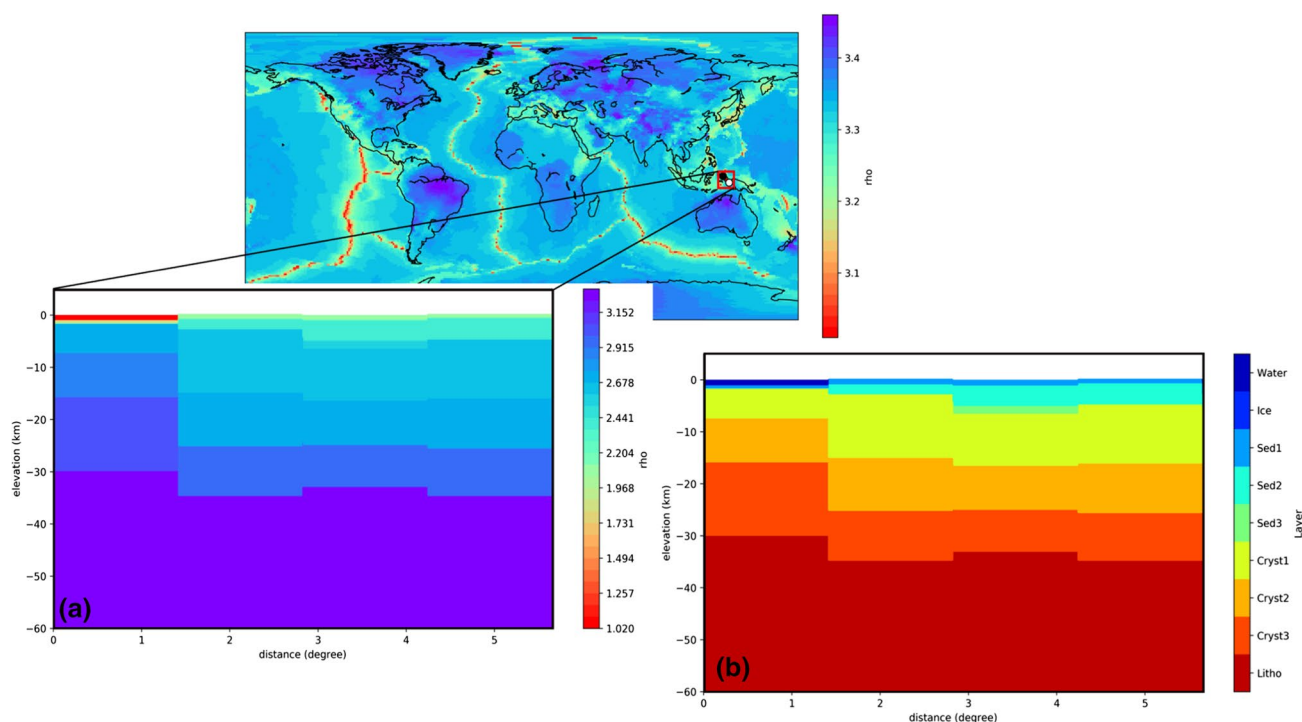


Fig. 6 CRUST 1.0 cross section in a West Papua, Indonesia: **a** subsurface density distribution; **b** the Earth's crust thickness

and northeastern seas, whereas high values founded on land with high topographic elevations in mountain ranges. The complete Bouguer anomaly is high in northern and eastern parts of the West Papua bird's head and is assumed to be part of the surface of the mantle or Moho layer, which is at a shallow depth with high rock density. This high anomaly is also connected to the subduction of the Pacific Ocean plate in the northern part associated with the Manokwari trough.

The complete Bouguer anomaly decreases in south and west, reaching a circular minimum in the neck of birds associated with the Bintuni Basin. The main components are composed of siliciclastic and sedimentary rocks in the Australian tectonic plate layer southeast of the Lunguru Fold Belt (LFTB). Low Bouguer anomalies are associated with positive elevations, while high anomalies are associated with negative elevations. This correlation exists because the Bouguer anomaly is directly related to the density distribution in the crust and mantle (Gushurst and Mahatsente 2020). The Bird's Head Formation is generally described as the northern and eastern Pacific Intra-island arc material, followed by the southern and western Australian continental material (Gold et al. 2017b). A low anomaly is also seen in the southwest part associated with the Seram trough in Maluku province, thought to be a subduction zone of the Papuan bird's head microplate under the Banda Sea (Putra and Husein 2019).

The Sorong fault line from west to east is the boundary between the Pacific oceanic crust in the north and the Australian continental crust in the south, according to the complete Bouguer anomaly map. A low Bouguer anomaly has been studied in relation to the low seismicity

parameter b , whereas the opposite is thought to be related to the offshore free air anomaly. Temporal variations in the value of b are interpreted as a result of seismicity migration by changes in spatial petrological, geophysical, and rheological characteristics (El-Isa and Eaton 2014). To emphasize the main regional geological structures in West Papua, including Koor, Sorong, Ransiki, and Yapen faults, a second radial derivative map is also analyzed based on the XGM2019e model. The value of the second radial derivative ranges from -184.93 Eotvos (mGal/km) to 364.80 Eotvos (mGal/km), as shown in Fig. 3c. On the second r derivative map, it is clear that the main fault structure paths in the study area tend to be associated with zero values. In this route, earthquakes predominantly occur in the province of West Papua.

The process is carried out to obtain regional anomalies and eliminate the influence of small structures from the gravity data in form of residual anomalies. Regional gravity anomalies are used as input data for gravity inversion modeling to obtain a basement model in the study area. The positive regional gravity anomaly ranged from 85.90 to 406.08 mGal (Fig. 7a), while the residual gravity anomaly ranged from -72.45 to 110.40 mGal (Fig. 7b). The high regional anomaly is located in the north of West Papua and decreases toward the south with a circular pattern at the neck of the associated bird in the Bintuni basin. Residual anomalies are more complex than regional anomalies, with a predominance of moderate to low values. The high residual anomaly is distributed in several places, especially on the Koor fault line in the north, the Sorong fault and the Ransiki fault in the southeast, it is

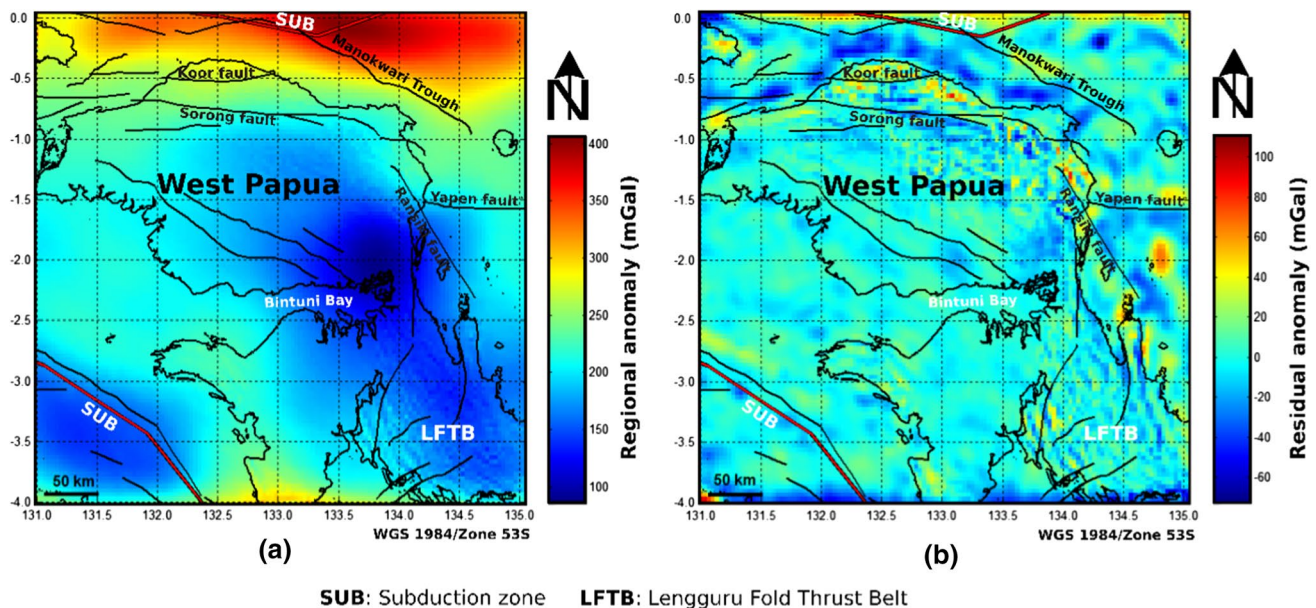


Fig. 7 Gravity anomalies separation in the West Papua region: **a** regional anomaly; **b** residual anomaly

thought to be related to the volcanic rock lithology which has a high density (Fig. 2). Regional gravity anomalies generally describe large and deep geological structures, while residual anomalies are associated with small and shallow structures.

Gravity gradient in West Papua

The gravity gradient study intends to enhance the boundaries of structures or geological contacts in West Papua that are not yet clearly evident on the complete Bouguer anomaly map. There are three gradient applications: vertical, horizontal, and tilt angle gradients. Vertical gradients range from

–20.97 to 19.61 mGal/km (Fig. 8a), where high anomalies are present in the north, while low anomalies are distributed in several locations such as the head and neck of birds to the south. The structure of the main fault and geological contacts in the study area are generally associated with zero values at vertical gradients.

Horizontal gradients varied from 0.039 to 16.56 mGal/km, with the largest amplitude value on the horizontal gradient map indicating the borders of geological contacts, significant faults, and important geological formations in the West Papua area (Fig. 8b).

Tilt angle gradient analysis is defined as the arcane value of the ratio of vertical and horizontal derivatives of gravity

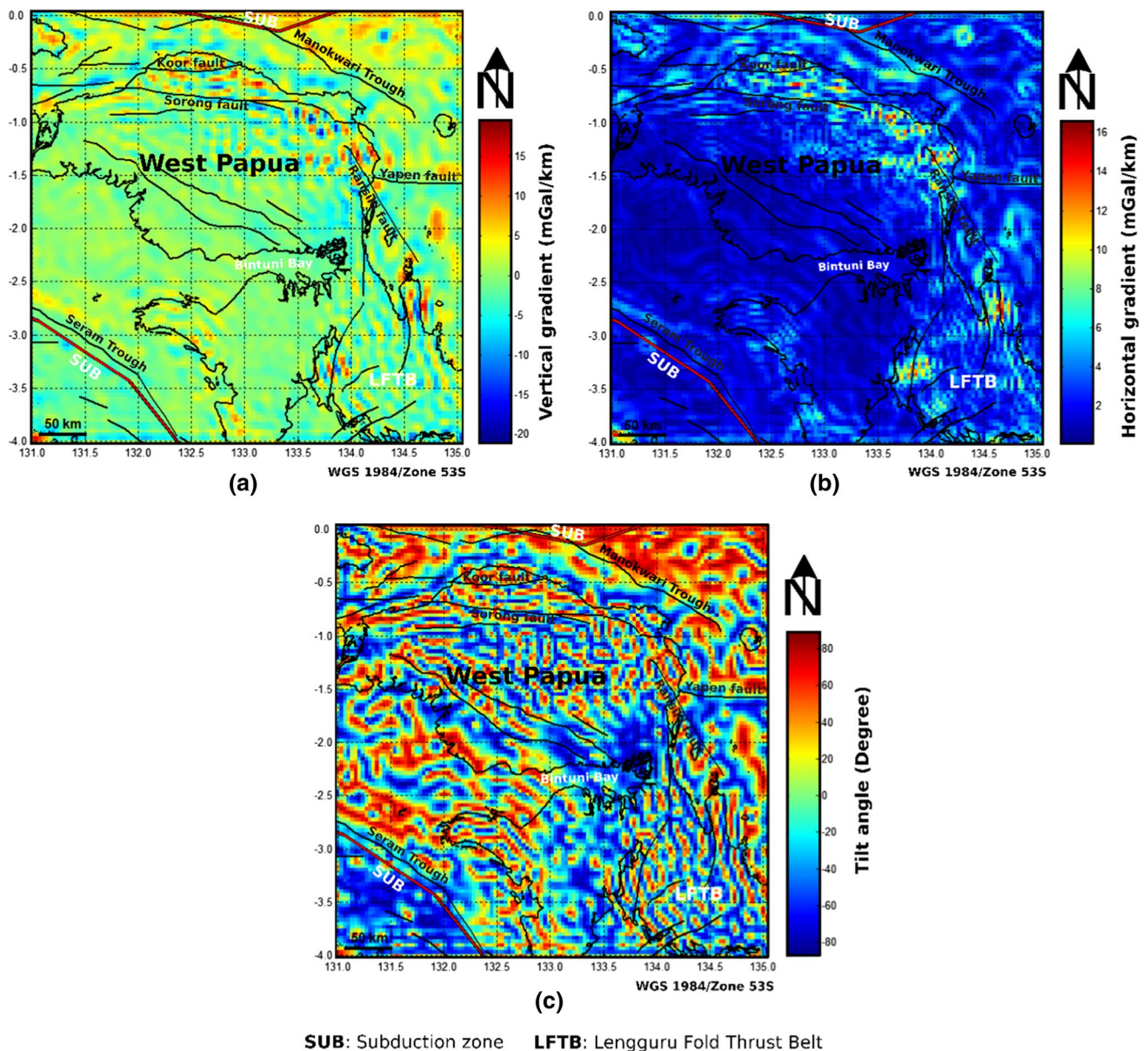


Fig. 8 Gravity gradient analysis in West Papua; **a** vertical gradient, **b** horizontal gradient, **c** tilt angle

anomalies. The advantage of tilt angle analysis when compared to other methods is that it does not require physical parameters such as density, magnetic susceptibility, inclination, structural index, etc. in its calculations (Akin et al. 2011). The tilt angle in West Papua ranges from -87.03° to 88.50° with a more complex pattern than vertical and horizontal gradients (Fig. 8c). Positive values predominate in the north, to the east, and in the west, while negative values are generally associated with the contact boundaries of geological structures and major faults in the study region. The zero value of the tilt angle expresses the vertical boundary of the anomalies source or geological structure.

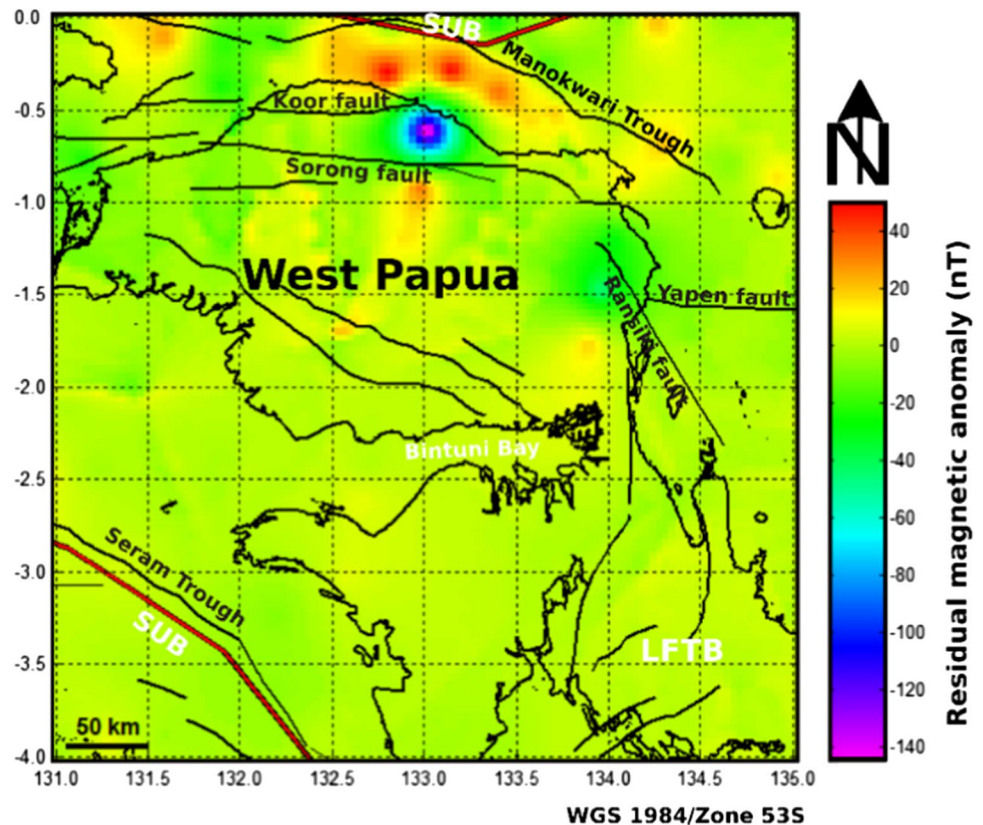
Magnetic anomaly in West Papua

The EMAG2-v3 model provides two types of magnetic anomaly data extracted for the West Papua region, including sea level anomalies and an upward continuation of 4 km above the sea level. The sea-level magnetic outliers ranged from -472.75 to 101.94 nT (Fig. 4a), while the upward continuation magnetic anomalies at 4 km altitude ranged from -328.178 to 62.001 nT (Fig. 4b). Overall, the magnetic anomaly patterns for both models are similar, with

high anomalies dominating in the north associated with the Manokwari Trough subduction zone, and high anomalies also seen at the bird's neck in the south. From west to east, low magnetic anomalies dominate Bird's Head, primarily along the Koor, Sorong, Ransiki, and Yapen strike-slip fault lines.

The high-to-low magnetic anomalies in both models suggest west-to-east subduction from the north of Bird's Head, a contribution from the Pacific Plate. Low negative anomalies with circular shapes were found on the main Sorong and Koor fault lines and at two locations on the Ransiki fault line in the South Manokwari District, possibly caused by igneous intrusions in the study area. Such low magnetic anomalies are generally associated with low rock susceptibility values in which volcanic rocks lose their magnetism from high temperature and high pressure. To further emphasize the magnetic anomalies that can describe smaller geological structures, residual anomalies were also calculated based on the difference between sea-level outliers and results that carried over up to 4 km. Residual outliers ranged from -144.57 to 49.86 nT (Fig. 9). The high residual anomaly further emphasizes the geological contact boundary indicating subduction in the northern part of the Papuan bird's head, associated with the Manokwari trough of Pacific oceanic crustal rocks.

Fig. 9 Residual magnetic anomalies are the difference from anomalies at sea level and upward continuation anomalies at an altitude of 4 km



SUB: Subduction zone

LFTB: Lengguru Fold Thrust Belt

Gravity and magnetic inversion

Subsurface model of rocks in the Province of West Papua as a function of density and magnetic susceptibility distribution are generated using inversion modeling of gravity and magnetic anomalies. Inversion has been used to iteratively update the model parameters to minimize the objective function, resulting in a fit between the prediction model and the observation data. The non-unique solution of the model can be determined and produced into a single model by minimizing the objective function of the model, which refers to the data fit (Li and Oldenburg 1996). The inversion problem in this study is underdetermined because the number of cells is much greater than

the amount of data used, where the total volume of the study area based on the results of gravity and magnetic inversion is 5.4 million km³. Gravity data inversion using the IRI method in the 13th iteration resulted in a fit data of 0.986 with a computational error tolerance of 0.002.

These findings are given in the form of comparisons between measurement data (Fig. 10a) and prediction or calculation data (Fig. 10b), as well as error models coming from those computational processes, which is the difference between prediction data and measurement data (Fig. 10c). Figure 10a, b shows a high match between the prediction data and the gravity observation data. The solution is provided by minimizing the global objective function consisting of the model objective function and data misfit (Li and

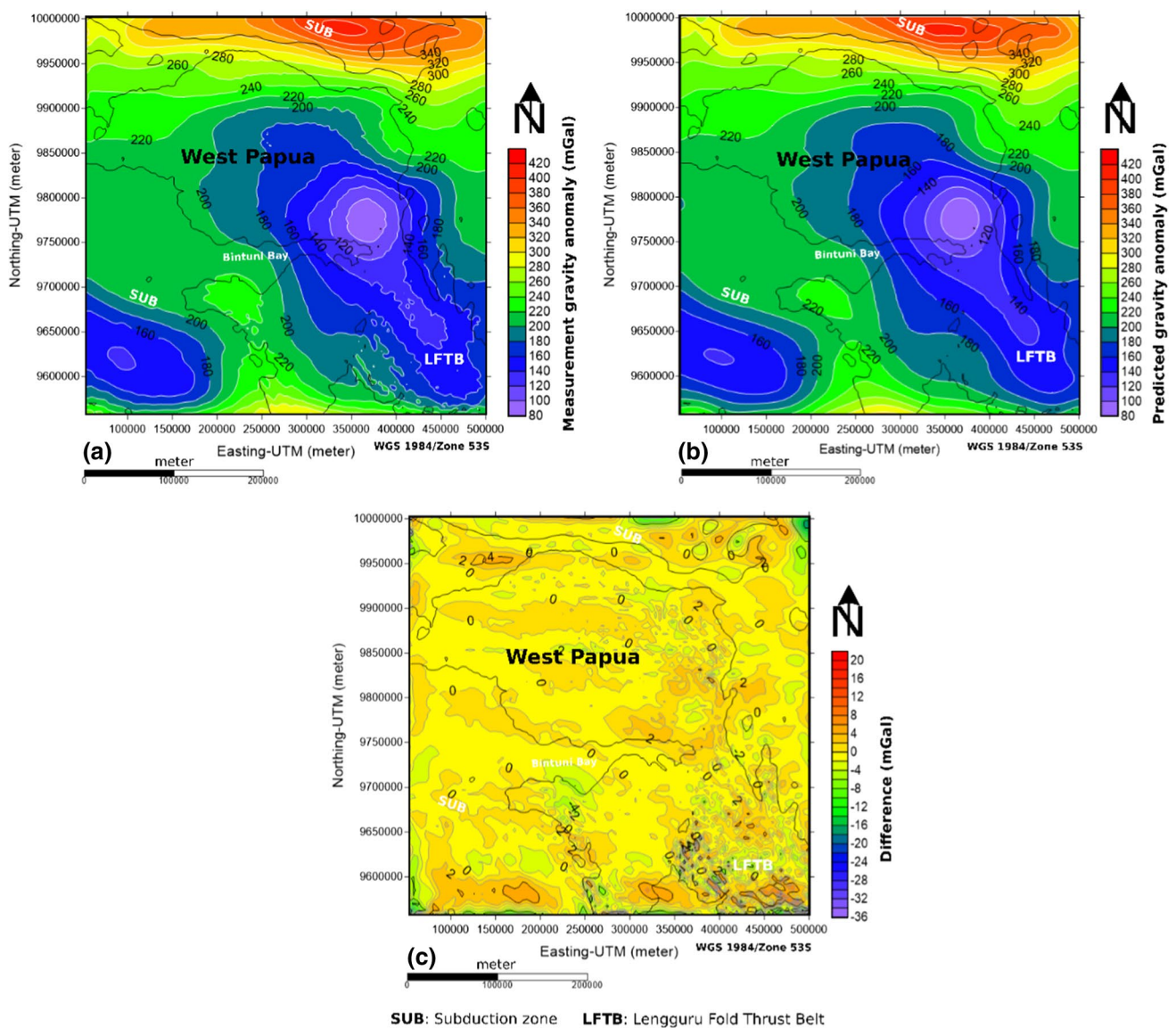


Fig. 10 The process of inversion of Earth gravity data in West Papua: **a** measurement data; **b** prediction data; **c** difference of measurement and prediction data

Oldenburg 1996, 1998). Data fit values on VOXI delivers misfit values adjusted by the number of data observation points. We discovered that the generated model is accurate and dependable to interpret since the data show a high fitting between the two anomalies data about values and shapes, with a disparity around of 2.282 mGal. Following the completion of the inversion operation, we constructed a subsurface model in West Papua as a function of rock density contrast.

In general, the findings of the subsurface model in the form of a density contrast distribution conform to the observation data pattern, where high values dominate in the north of the bird's head and low values dominate on the bird's neck.

Subsurface rock density contrast ranging from -0.348 to 0.451 gr/cm^3 , displayed in the form of overlaid at various depths of 5 km (Fig. 11a), 10 km (Fig. 11b), 15 km (Fig. 11c), and 20 km (Fig. 11d). It provides a low to medium rock density contrast at a depth of 5 km, with low values recorded in many sites in the northern, bird's neck, southwest, and southeast. The low density contrast is assumed to be caused by tectonic activity in the research region. Major fault geological features, such as the Sorong, Koor, Ransiki, and Yapen faults, are found along the boundaries of low and high density contrast, particularly in the northern part of the bird's head from west to east.

The low-density contrast in the bird's neck is directly tied to the Bintuni basin, which is the largest oil and gas producing basin in eastern Indonesia. The basement rock of

this basin is the Silur-Devon (Paleozoic) Kemum formation, which consists of clay rocks, graywackes, and coarse clastic. The Kemum formation is assumed to have been formed by granite rock slides and intrusion (Handyarso and Padmawidjaja 2017). High-density contrast dominates the whole research region at a depth of 10 km. The Bintuni basin arises clearly in this layer, with a low-density difference between high rock density. In general, rock density contrast at depths of 15 and 20 km follows the same pattern, with high-density contrast dominating overall. This layer is assumed to be the boundary between the sediment layer and the upper crust, which is considered to be a basement layer in the research region when combined with CRUST 1.0 model of West Papua (Fig. 6).

To support the results of 3-D inversion of gravity data, inversion modeling of the 4 km upward continuation of magnetic data has been conducted based on the EMAG2-v3 model. Similar to gravity data inversion, the results of a 3-D magnetic inversion are presented in the form of a comparison between the measurement data (Fig. 12a) and the prediction model (Fig. 12b), as well as the resulting difference between the two data (Fig. 12c). There is a high match between measurement data and prediction data with relatively small misfit, magnetic inversion using the IRI approach in the 11th iteration resulted in a data fit of 1.0249 with a computational error tolerance of 0.002. The absolute fit error value of the data is 2.008 nT. The subsurface model in the form of the rock's magnetic susceptibility distribution

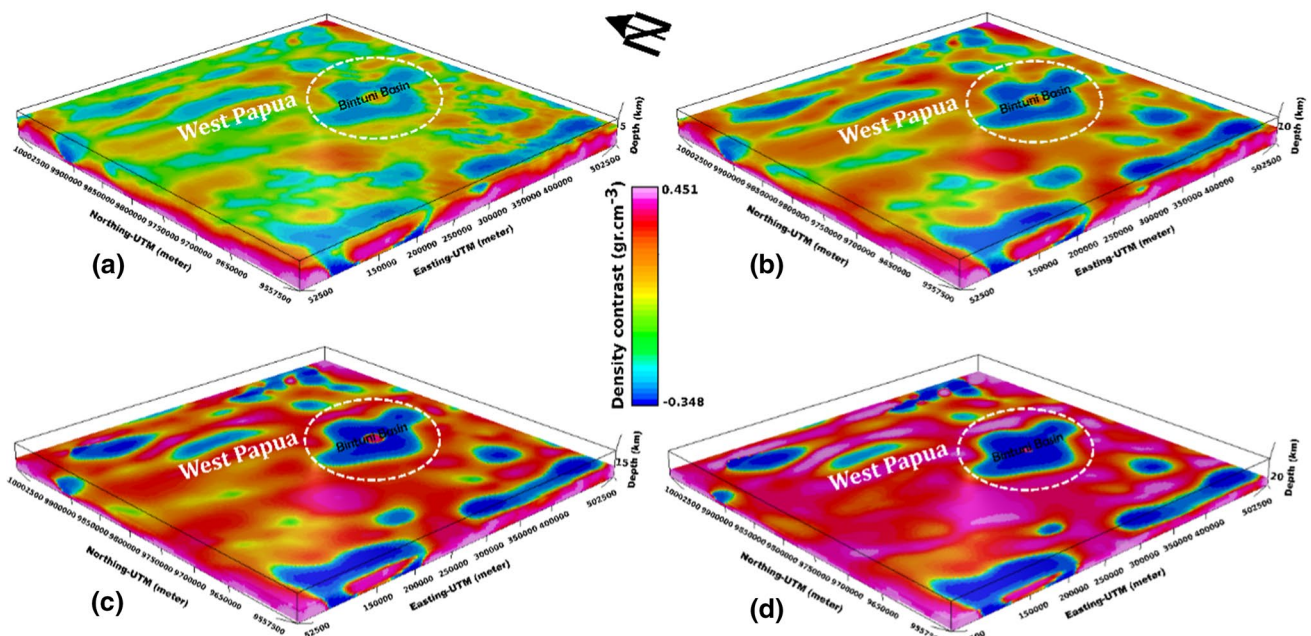


Fig. 11 Model of rock density at various depths in West Papua based on regional gravity anomaly 3-D inversion: **a** 5 km; **b** 10 km; **c** 15 km; and **d** 20 km

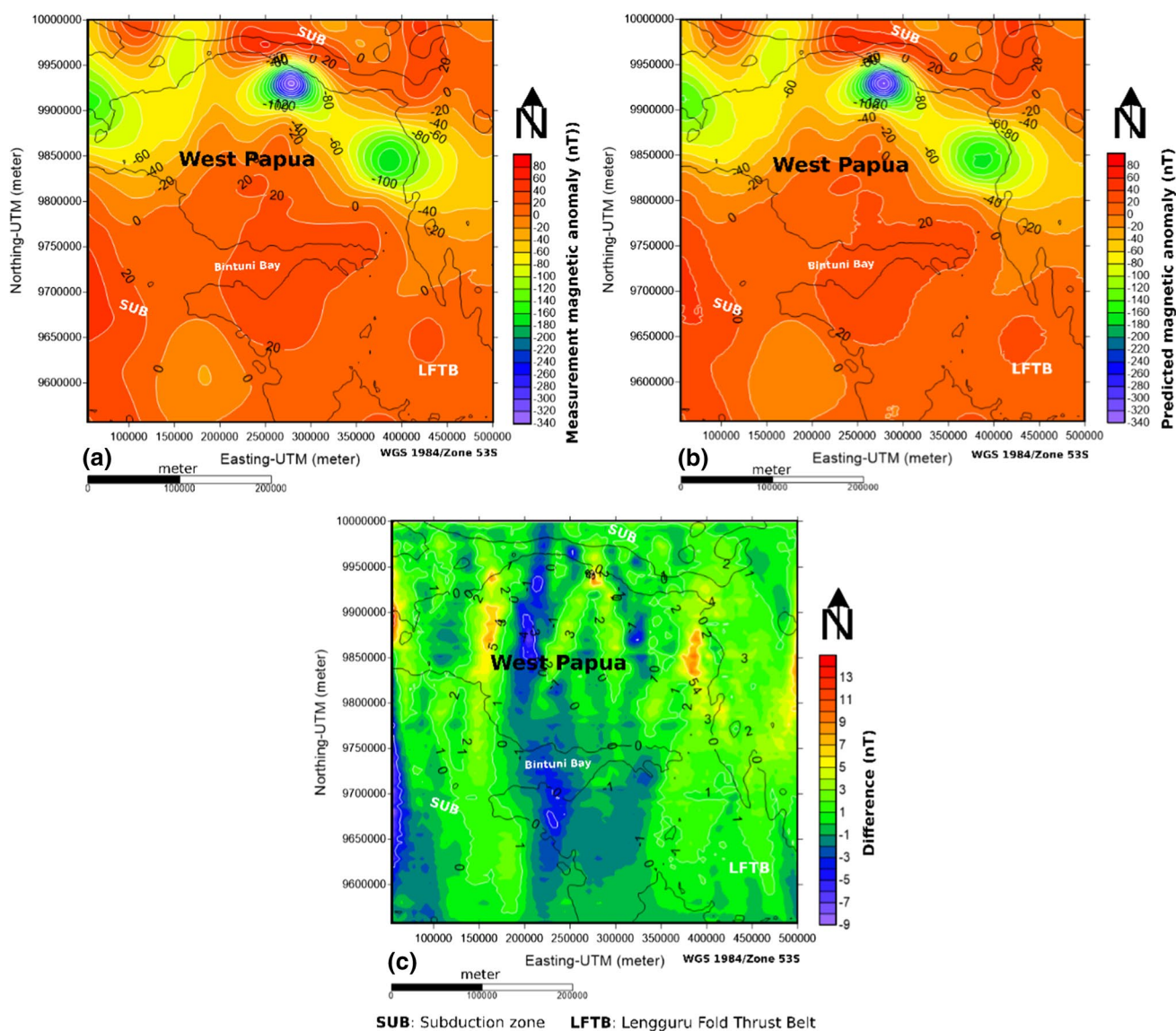


Fig. 12 The process of inversion of magnetic data in West Papua: **a** measurement data; **b** prediction data; **c** difference of measurement and prediction data

should be valid to be interpreted due to the value and shape of both magnetic anomalies after inversion.

The physical parameter value of magnetic susceptibility resulting from inversion ranges from -0.363 to 0.223 SI. In this case, the inversion used is an unconstrained inversion because the study area is quite wide and the magnetic anomaly is dominated by negative anomalies without prior leveling, so it is not limited to the magnetic susceptibility value of subsurface rocks as a constraint. Negative susceptibility is thought to be associated with materials with high diamagnetic properties in the study area or generated by mathematical and/or physical processes that result in non-unique properties of the model because the inversion is performed freely. The susceptibility layering system is shown

in depth variations as is the case in gravity data inversion. Magnetic susceptibility at a depth of 5 km has a more complex pattern dominated by moderate to high susceptibility in the northern and southern parts, while low susceptibility is found in the middle or bird neck of study area (Fig. 13a). High susceptibility is seen dominantly in the north and south at a depth of 10 km (Fig. 13b), while susceptibility at 15 km (Fig. 13c) and 20 km (Fig. 13d) generally regards the same pattern, with high susceptibility in the northern part toward the west to east and the south of the central part.

The high susceptibility is assumed to be due to the presence of magnetic materials in the Pacific Ocean crust, which also has a high rock density. This layer is thought to be West Papua's basement layer. Bintuni basins, which are rich in oil

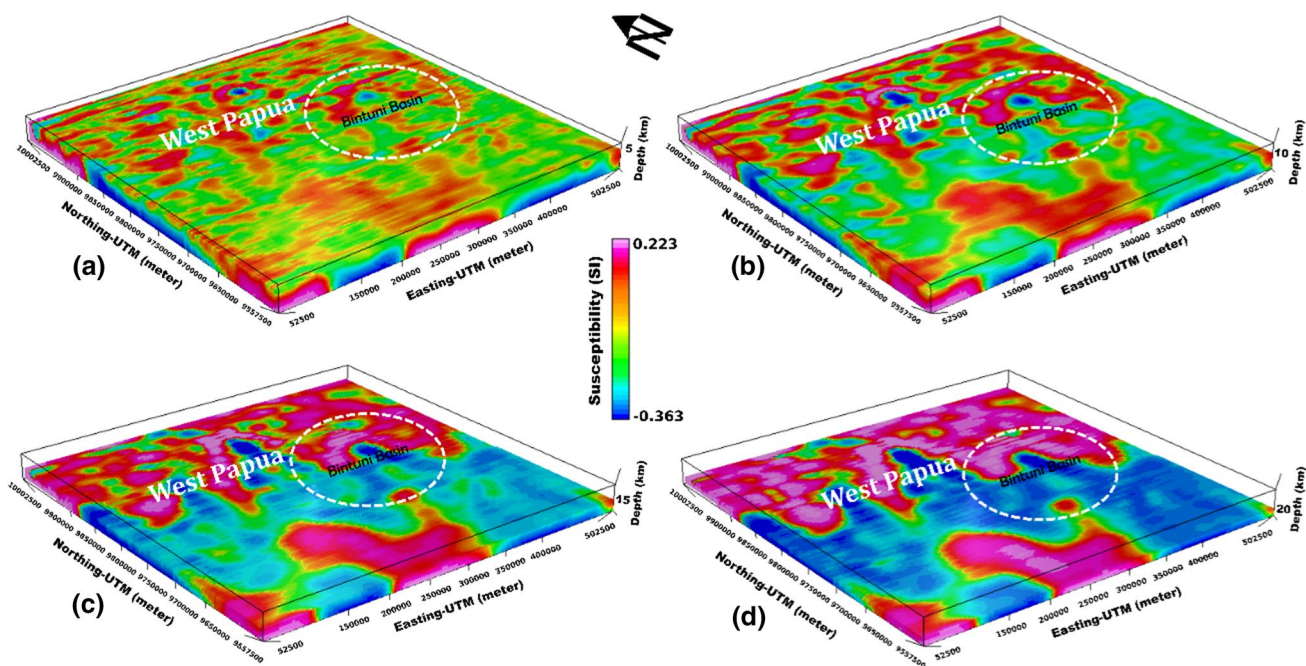


Fig. 13 Model of rock susceptibility at various depths in West Papua based on regional magnetic anomaly 3-D inversion: **a** 5 km; **b** 10 km; **c** 15 km; and **d** 20 km

and gas, often have low rock susceptibility due to quarter and siliciclastic sediment layers. Low to negative susceptibility is thought to be associated with materials with high diamagnetic properties in the study area.

To indicate the presence of tectonic activity in the region of West Papua, a subsurface model comparing the density

and susceptibility of rocks is displayed in the form of a cross section across the north–south direction of a 3-D inversion (Fig. 14). Figure 14a shows a 2-D cross section of gravity data inversion demonstrating the subduction of the Pacific plate with a high rock density contrast under the Australian continental plate with a lower density contrast from the

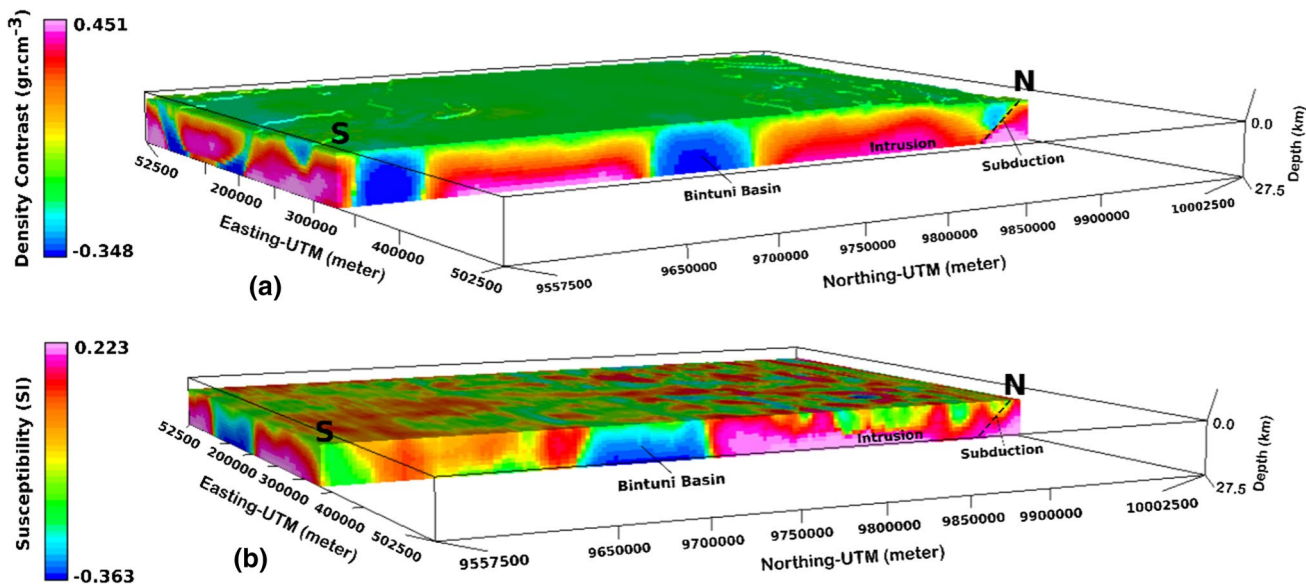


Fig. 14 North to south cross-sectional model showing the subduction pattern of the Pacific plate beneath the Australian plate in West Papua: **a** gravity inversion; **b** magnetic inversion results

north. It may also be evident in the pattern of granite rock intrusion, particularly in mountain ranges in the research area. Past volcanic activity in the heads of Papuan birds was intense during the Triassic period, with evidence of granite found at various spots in the bird's head and western part, and also southwest of Cenderawasih bay. The granite is part of the Netoni intrusion complex, and so are Anggi granite, Wariki granodiorite, and Warjori granite (Gold et al. 2017b; Webb and White 2016). In the gravity inversion cross section, it is also clearly visible Bintuni basin with negative density contrast, allegedly rich in oil and gas potential in the region.

Figure 14b depicts a 2-D cross section of magnetic inversion, which shows the presence of the same pattern as the Earth's gravitational inversion. Subduction of the Pacific plate is defined by the existence of strong rock susceptibility beneath the Australian continental plate with lower susceptibility. The existence of granite intrusion is also illustrated through models with high susceptibility. A cross section of gravity and magnetic data inversions showed corresponding results related to subsurface geological structures in West Papua province.

Conclusion

The utilization and analysis of gravity and magnetic data from satellite observations based on the 2012 WGM and EMAG2-v3 models provide significant information for the study of tectonic activity and the determination of subsurface structures in West Papua, Indonesia. The utilization and analysis of gravity and magnetic data from satellite observations based on the 2012 WGM and EMAG2-v3 models provide significant information for the study of tectonic activity and the determination of subsurface structures in West Papua, Indonesia. High gravity and magnetic anomalies in the north are assumed to be mostly produced by igneous rocks as a result of the subduction of the high-density Pacific Oceanic plate, as well as the upper mantle rich in magnetic materials beneath the continental crust of Australia. Low gravity and magnetic anomalies in the neck of birds are considered to represent weak zones generated by the convergence of tectonic plates in the main basin of Bintuni, which is rich in oil and gas.

The evaluation of gradients or gravity field derivatives enhances and improves the boundaries of major geological structures such as the Sorong, Koor, Ransiki, and Yapen faults, which are the paths of earthquakes in West Papua. Quantitative interpretation through unconstrained 3-D iterative reweighting inversion of regional gravity and magnetic anomalies provides corresponding results in the form of a high density contrast and magnetic susceptibility in the northern part related to subduction of the Pacific Ocean plate

and igneous rock intrusion. Low density and susceptibility contrast is related to the dominance of sedimentary rocks and also the presence of more diamagnetic properties of oil and gas potential in the Bintuni basin. The depth of the bedrock layer (basement) is estimated to be between 15 and 20 km with rocks from the mantle in the northern part as the basement, and the Kemum formation consisting of siliciclastic metamorphic rocks aged Silur-Devon in the south. Our research is limited to unconstrained inversions based on the availability of gravity and magnetic satellite data, so further direct measurements are needed in the field for narrower regions using constraint inversion.

Acknowledgements The author would like to thank Gadjah Mada University for providing the opportunity to participate in the 2021 post-doctoral program with grant number: 6144/UN1.P.III/DIT-LIT/PT/2021. The authors also thank the International Bureau of Gravity Survey (BGI) for the WGM 2012 gravity data and the National Oceanic and Atmospheric Administration (NOAA) for the EMAG2-V3 data, which are freely accessible for research. Thanks are due also to Seequent for the opportunity to model the inversion of gravity and magnetic data in West Papua using the Oasis Montaj 9.10 software.

Author contributions R.L has developed the research concepts and designs, as well as written the manuscript. S.S. writes and assesses research findings in the form of a published manuscript. L.L helps in the similarity checking process and also for changes and improvements to the English language of the manuscript.

Data availability The datasets used in this study are available upon reasonable request from the corresponding author.

Declarations

Conflict of interest The authors state that they do not have any competing interests.

References

- Abderbi J, Khattach D, Kenafi J (2017) Multiscale analysis of the geophysical lineaments of the High Plateaus (Eastern Morocco): structural implications. *J Mat Environ Sci* 8(2):467–475
- Afshar A, Norouzi G-H, Moradzadeh A, Riahi M-A (2018) Application of magnetic and gravity methods to the exploration of sodium sulfate deposits, case study: Garmab mine, Semnan, Iran. *J Appl Geophys* 159:586–596. <https://doi.org/10.1016/j.jappgeo.2018.10.003>
- Akin U, Şerifoğlu Bİ, Duru M, (2011) The use of tilt angle in gravity and magnetic methods. *Bull Miner Res Explor* 143(143):1–12
- Baldwin SL, Fitzgerald PG, Webb LE (2012) Tectonics of the New Guinea region. *Annu Rev Earth Planet Sci* 40(1):495–520. <https://doi.org/10.1146/annurev-earth-040809-152540>
- Balmino G, Vales N, Bonvalot S, Briais A (2012) Spherical harmonic modelling to ultra-high degree of Bouguer and isostatic anomalies. *J Geodesy* 86(7):499–520. <https://doi.org/10.1007/s00190-011-0533-4>
- Charlton TR (2010) The Pliocene-recent anticlockwise rotation of the Bird's head, the opening of the Aru Trough—Cendrawasih Bay Sphenochasm, and the Closure of the Banda Double Arc. <http://>

- archives.datapages.com/data/ipa_pdf/081/081001/pdfs/IPA10-G-008.htm
- Daniarsyad G, Suardi I (2017) Stress triggering among $MW \geq 6.0$ significant earthquakes in Manokwari Trough. *AIP Conf Proc* 1857(1):020014. <https://doi.org/10.1063/1.4987056>
- Dentith MC, Mudge ST (2014) *Geophysics for the mineral exploration geoscientist*. Cambridge University Press, Cambridge
- El-Isa ZH, Eaton DW (2014) Spatiotemporal variations in the b-value of earthquake magnitude–frequency distributions: classification and causes. *Tectonophysics* 615–616:1–11. <https://doi.org/10.1016/j.tecto.2013.12.001>
- Ellis RG, MacLeod IN (2013) Constrained voxel inversion using the Cartesian cut cell method. *ASEG Ext Abstr* 2013(1):1–4. <https://doi.org/10.1071/ASEG2013ab222>
- Eshaghzadeh A, Dehghanpour A, Kalantari RA (2018) Application of the tilt angle of the balanced total horizontal derivative filter for the interpretation of potential field data. *Bollettino Di Geofisica Teorica Ed Applicata* 59(2):161–178. <https://doi.org/10.4430/bgta0233>
- Gold DP, Burgess PM, BouDagher-Fadel MK (2017a) Carbonate drowning successions of the Bird's Head, Indonesia. *Facies* 63(4):25. <https://doi.org/10.1007/s10347-017-0506-z>
- Gold DP, White LT, Gunawan I, BouDagher-Fadel MK (2017b) Relative sea-level change in western New Guinea recorded by regional biostratigraphic data. *Mar Petroleum Geol* 86:1133–1158. <https://doi.org/10.1016/j.marpetgeo.2017.07.016>
- Gómez-García ÁM, Meeßen C, Scheck-Wenderoth M, Monsalve G, Bott J, Bernhardt A, Bernal G (2019) 3-D Modeling of vertical gravity gradients and the delimitation of tectonic boundaries: the Caribbean oceanic domain as a case study. *Geochem Geophys Geosyst* 20(11):5371–5393. <https://doi.org/10.1029/2019GC008340>
- Gushurst G, Mahatsente R (2020) Lithospheric structure of the Central Andes Forearc from gravity data modeling: implication for plate coupling. *Lithosphere* 2020(1):8843640. <https://doi.org/10.2113/2020/8843640>
- Handyarso A, Padmawidjaja T (2017) Struktur Geologi Bawah Permukaan Cekungan Bintuni Berdasarkan Data Gaya Berat. *Jurnal Geologi Dan Sumberdaya Mineral* 18(2):53–65. <https://doi.org/10.33332/jgsm.geologi.v18i2.125>
- Hinze WJ, von Frese RRB, Saad AH (2013) *Gravity and magnetic exploration: principles, practices, and applications*. Cambridge University Press. <https://doi.org/10.1017/CBO9780511843129>
- Ibraheem IM, Haggag M, Tezkan B (2019) Edge detectors as structural imaging tools using aeromagnetic data: a case study of Sohag Area, Egypt. *Geosciences* 9(5):211. <https://doi.org/10.3390/geosciences9050211>
- Ince ES, Barthelmes F, Reißland S, Elger K, Förste C, Flechtner F, Schuh H (2019) ICGEM—15 years of successful collection and distribution of globalgravitational models, associated services and future plans. *Earth Syst Sci Data* 11(2):647–674. <https://doi.org/10.5194/essd-2019-17>
- Ingram DM, Causon DM, Mingham CG (2003) Developments in Cartesian cut cell methods. *Math Comput Simul* 61(3):561–572. [https://doi.org/10.1016/S0378-4754\(02\)00107-6](https://doi.org/10.1016/S0378-4754(02)00107-6)
- Kalaneh S, Agh-Atabai M (2016) Spatial variation of earthquake hazard parameters in the Zagros fold and thrust belt, SW Iran. *Nat Hazards* 82(2):933–946. <https://doi.org/10.1007/s11069-016-2227-y>
- Laske G, Masters G, Ma Z, Pasyanos M (2013) Update on CRUST1.0—A 1-degree global model of Earth's crust. In: *Abstract EGU2013-2658* Presented at 2013 Geophys. Res. Abstracts, vol 15, no 15, p 2658
- Lewerissa R, Sismanto S, Setiawan A, Pramumijoyo S (2020) The igneous rock intrusion beneath Ambon and Seram islands, eastern Indonesia, based on the integration of gravity and magnetic inversion: its implications for geothermal energy resources. *Turkish J Earth Sci* 29(4):596–616. <https://doi.org/10.3906/yer-1908-17>
- Lewerissa R, Rumahey R, Syakur YA, Laponi L (2021) Completeness magnitude (M_c) and b-value characteristics as important parameters for future seismic hazard assessment in the West Papua province Indonesia. *Arab J Geosci* 14(23):2588. <https://doi.org/10.1007/s12517-021-08885-4>
- Li Y, Oldenburg DW (1996) 3-D inversion of magnetic data. *Geophysics* 61(2):394–408. <https://doi.org/10.1190/1.1443968>
- Li Y, Oldenburg DW (1998) 3-D inversion of gravity data. *Geophysics* 63(1):109–119. <https://doi.org/10.1190/1.1444302>
- Makrup L, Hariyanto A, Winarno S (2018) Seismic Hazard Map for Papua Island. *Int Rev Civ Eng (IRECE)* 9:57. <https://doi.org/10.15866/irece.v9i2.14090>
- Maus S, Barckhausen U, Berkenbosch H, Bournas N, Brozena J, Childers V, Dostaler F, Fairhead JD, Finn C, von Frese RRB, Gaina C, Golynsky S, Kucks R, Lühr H, Milligan P, Mogren S, Müller RD, Olesen O, Pilkington M, Saltus R, Schreckenberger B, Caratori Tontini F (2009) EMAG2: a 2-arc min resolution Earth Magnetic Anomaly Grid compiled from satellite, airborne, and marine magnetic measurements. *Geochem Geophys Geosyst* 10(8). <https://doi.org/10.1029/2009GC002471>
- Meyer B, Chulliat A, Saltus R (2017) Derivation and Error analysis of the earth magnetic anomaly grid at 2 arc min resolution version 3 (EMAG2v3). *Geochem Geophys Geosyst* 18(12):4522–4537. <https://doi.org/10.1002/2017GC007280>
- Milsom J (1991) Gravity measurements and terrane tectonics in the New Guinea region. *J Southeast Asian Earth Sci* 6(3–4):319–328. [https://doi.org/10.1016/0743-9547\(91\)90077-B](https://doi.org/10.1016/0743-9547(91)90077-B)
- Milsom J, Masson D, Nichols G, Sikumbang N, Dwiyanto B, Parson L, Gallagher H (1992) The Manokwari Trough and the western end of the New Guinea Trench. *Tectonics* 11(1):145–153. <https://doi.org/10.1029/91TC01257>
- Oldenburg DW, Li Y (1994) Subspace linear inverse method. *Inverse Prob* 10(4):915–935. <https://doi.org/10.1088/0266-5611/10/4/011>
- Oldenburg D, Li Y (2005) 5. Inversion for applied geophysics: a tutorial. *Near Surf Geophys*. <https://doi.org/10.1190/1.9781560801719.ch5>
- Putra A, Husein S (2019) Regional overview of orogenic belts in Indonesia: emphasis on the occurrences of thrust wedge systems. *Berita Sedimentologi* 44:19–41
- Reynolds JM (1997) *An introduction to applied and environmental geophysics*. John Wiley, London
- Saibi H, Hag DB, Alamri MSM, Ali HA (2021) Subsurface structure investigation of the United Arab Emirates using gravity data. *Open Geosci* 13(1):262–271. <https://doi.org/10.1515/geo-2020-0233>
- Serhalawan YR, Sianipar DSJ (2017) Pemodelan Mekanisme Sumber Gempa Bumi Ransiki 2012 Berkekuatan MW 6, 7. *JST (jurnal Sains Dan Teknologi)* 6(1):10
- Shandini Y, Kouske PA, Nguiya S, Marcelin MP (2018) Structural setting of the Koum sedimentary basin (north Cameroon) derived from EGM2008 gravity field interpretation. *Contrib Geophys Geodesy* 48(4):281–298. <https://doi.org/10.2478/congeo-2018-0013>
- Soulaimani S, Chakiri S, Manar A, Soulaimani A, Miftah A, Bouiflane M (2020) Potential-field geophysical data inversion for 3D modelling and reserve estimation (Example of the Hajjar mine, Guemassa massif, Morocco): magnetic and gravity data case. *Comptes Rendus Géoscience* 352(2):139–155. <https://doi.org/10.5802/crgeos.10>
- Tian T, Zhang J, Jiang W, Tian Y (2020) Quantitative study of crustal structure spatial variation based on gravity anomalies in the Eastern Tibetan Plateau: Implication for earthquake susceptibility

- assessment. *Earth Space Sci* 7(3):e2019EA000943. <https://doi.org/10.1029/2019EA000943>
- Watkinson IM, Hall R (2017) Fault systems of the eastern Indonesian triple junction: evaluation of quaternary activity and implications for seismic hazards. *Geol Soc Lond Special Publ* 441(1):71–120. <https://doi.org/10.1144/SP441.8>
- Webb M, White L (2016) Age and nature of Triassic magmatism in the Netoni Intrusive Complex, West Papua, Indonesia. *J Asian Earth Sci*. <https://doi.org/10.1016/j.jseaes.2016.09.019>
- Zeng H, Xu D, Tan H (2007) A model study for estimating optimum upward-continuation height for gravity separation with application to a Bouguer gravity anomaly over a mineral deposit, Jilin province, northeast China. *Geophysics* 72(4):I45–I50. <https://doi.org/10.1190/1.2719497>
- Zingerle P, Pail R, Gruber T, Oikonomidou X (2020) The combined global gravity field model XGM2019e. *J Geodesy*. <https://doi.org/10.1007/s00190-020-01398-0>

Springer Nature or its licensor holds exclusive rights to this article under a publishing agreement with the author(s) or other rightsholder(s); author self-archiving of the accepted manuscript version of this article is solely governed by the terms of such publishing agreement and applicable law.